



CISTER

Research Center in
Real-Time & Embedded
Computing Systems

Technical Report

Reliable and fast hand-offs in low-power wireless networks

Hossein Fotouhi*

Mário Alves*

Marco Zuniga

Anis Koubâa*

*CISTER Research Center

CISTER-TR-140501

26, Sep, 2014

Reliable and fast hand-offs in low-power wireless networks

Hossein Fotouhi*, Mário Alves*, Marco Zuniga, Anis Koubâa*

*CISTER Research Center

Polytechnic Institute of Porto (ISEP-IPP)

Rua Dr. António Bernardino de Almeida, 431

4200-072 Porto

Portugal

Tel.: +351.22.8340509, Fax: +351.22.8340509

E-mail: mohfg@isep.ipp.pt, mjf@isep.ipp.pt, aska@isep.ipp.pt

<http://www.cister.isep.ipp.pt>

Abstract

Hand-off (or hand-over), the process where mobile nodes select the best access point available to transfer data, has been well studied in wireless networks. The performance of a hand-off process depends on the specific characteristics of the wireless link. In the case of low-power wireless networks, hand-off decisions must be carefully taken by considering the unique properties of inexpensive low-power radios. This article addresses the design, implementation and evaluation of smart-HOP, a hand-off mechanism tailored for low-power wireless networks. This work has three main contributions. First, it formulates the hard hand-off process for low-power networks (such as typical wireless sensor networks -WSNs) with a probabilistic model, to investigate the impact of the most relevant channel parameters through an analytical approach. Second, it confirms the probabilistic model through simulation and further elaborates on the impact of several hand-off parameters. Third, it fine-tunes the most relevant hand-off parameters via an extended set of experiments, in a more realistic experimental scenario. The evaluation shows that smart-HOP performs well in the transitional region while achieving more than 98% relative delivery ratio and hand-off delays in the order of a tenth of a second.

Reliable and fast hand-offs in low-power wireless networks

Hossein Fotouhi, Mário Alves, Marco Zúñiga, and Anis Koubâa,

Abstract—Hand-off (or hand-over), the process where mobile nodes select the best access point available to transfer data, has been well studied in wireless networks. The performance of a hand-off process depends on the specific characteristics of the wireless links. In the case of low-power wireless networks, hand-off decisions must be carefully taken by considering the unique properties of inexpensive low-power radios. This article addresses the design, implementation and evaluation of smart-HOP, a hand-off mechanism tailored for low-power wireless networks. This work has three main contributions. First, it formulates the hard hand-off process for low-power networks (such as typical wireless sensor networks - WSNs) with a probabilistic model, to investigate the impact of the most relevant channel parameters through an analytical approach. Second, it confirms the probabilistic model through simulation and further elaborates on the impact of several hand-off parameters. Third, it fine-tunes the most relevant hand-off parameters via an extended set of experiments, in a realistic experimental scenario. The evaluation shows that smart-HOP performs well in the transitional region while achieving more than 98% relative delivery ratio and hand-off delays in the order of a few tens of a milliseconds.

Index Terms—Mobility, Low-power links, Wireless sensor networks, Link characteristics, hand-off, hand-over.

1 INTRODUCTION

WIRELESS technologies have been key enabler for an expanding range of mobile applications, building not only on smart phones and tablets, but also on wearable sensors, industrial machinery, health-monitoring instruments and robotics [1]. These devices play an instrumental role in many new application domains that push wireless networks to dramatically improve quality-of-service properties such as throughput, timeliness, reliability, security, privacy, usability, and efficiency [1]–[3]. These QoS requirements must be guaranteed between mobile nodes and also between mobile nodes and fixed network infrastructures.

A recent NSF report [1] presents an exemplary scenario capturing this situation. In the future, in-body sensors collecting “*aggregated data from the entire population can predict outbreaks of epidemics even before they occur*” and it further states that “*such applications require in-body sensors that not only have robust wireless connectivity, but also are highly energy-efficient*”. We can easily foresee a hospital covered by a wireless sensor network (WSN) infrastructure (used for one or more purposes). Patients use body sensor networks to monitor relevant/vital signs—they are monitored and tracked either when standing still or moving (walking, wheel chair or in bed). Doctors and medical staff also use body sensor networks, which can be used to measure their stress/anxiety levels and also

to track and warn them about emergency situations. Only if these wearable body sensor nodes are able to communicate reliably and in real-time, this will effectively transform medical services in the near future.

In industrial environments such as factory automation and process control, it is essential to monitor the actual state of components and machines in a continuous manner. The Factories of the Future 2020 roadmap [2] forecasts “*the need for advanced machine interaction with humans through ubiquity of mobile devices to receive relevant production information*”. Such type of systems is also expected to detect potentially dangerous conditions in real-time and launch necessary countermeasures to prevent their impact on workers’ health and safety.

The Cooperating Objects roadmap [3] envisions and outlooks several application domains requiring the cooperation between mobile robots instrumented with sensing/actuation capabilities with fixed wireless sensor nodes, such as for search & rescue, environment exploration and surveillance applications. A large number of small (and inexpensive) robots can cooperate to tackle a large problem. These swarms of robots pose important challenges to robot designers as their cooperative behavior is not as simple to program as a single robot: many algorithms are distributed and rely heavily on communication between the participating members of the swarm and also with a fixed wireless infrastructure. Typically, this communication is time-critical, meaning it has to be completed within a time deadline to be effective.

Many recent research projects (e.g. [4]–[7]) and research works (e.g. [8]–[12]) have considered network architectures that require real-time (or at least continuous) data collection from mobile nodes through low-power wireless interfaces to fixed network infrastructures. In oil refineries, workers are exposed to hazardous environments in highly critical areas, so collecting the workers’ vital signs during their daily activity enables to quickly detect abnormal sit-

- Hossein Fotouhi and Mário Alves are with the CISTER/INESC-TEC, ISEP, Polytechnic Institute of Porto, Portugal.
E-mails: (mohfg,mjf)@isep.ipp.pt
- Marco Zúñiga is with the Embedded Software Group, Delft University of Technology, The Netherlands.
E-mail: m.a.zunigazamalloa@tudelft.nl
- Anis Koubâa is with the CISTER/INESC-TEC, ISEP, Polytechnic Institute of Porto, Portugal and COINS Research Group, Prince Sultan University, Saudi Arabia.
E-mail: aska@isep.ipp.pt

uations [8]. In clinical monitoring, patients have embedded sensing devices that report real-time streams of information through a fixed infrastructure [9], [10]. Mobile robots are also used to assist fixed sensor network deployments in wildlife monitoring to detect and extinguish fire [11], [12].

The communication between mobile nodes and a fixed infrastructure has been extensively studied in Cellular and WiFi networks, and it has been addressed through the use of hand-off mechanisms. However, these methods cannot be readily applied to low-power wireless networks [13]. First, Cellular and WiFi networks have more sophisticated radios with more energy resources. This means that their wireless links are much longer and more reliable than those provided by low-power low-cost radios, and hence the thresholds and parameters associated to hand-off mechanisms need to be tuned accordingly. Second, base stations in cellular networks build on fixed wired infrastructures with strong processing and communication capabilities, which is usually not applicable in low-power networks. Third, mobile nodes in Cellular and WiFi networks are usually in the coverage range of several strong radios while the unreliable links of low-power wireless networks have little overlap.

In this paper we address the design, implementation and evaluation of smart-HOP, a hand-off mechanism that considers the specific features of low-power links to enable fast, reliable and efficient hand-offs¹. We enhance our preliminary work published at [13] with the following new contributions:

- 1) We formulate a hard hand-off process for low-power networks with a probabilistic model to study the impact of relevant channel parameters.
- 2) We design a simulation model to confirm the probabilistic analysis and also to analyze the impact of relevant network parameters on the overall performance.
- 3) We further fine-tune the hand-off parameters through an extensive set of experiments in a realistic environment with a person holding the mobile node.

Organization. In Section 2, we explain the main limitations of low-power networks and overview some hand-off approaches for low-power wireless networks. In the remainder of the paper, the terms low-power wireless networks and wireless sensor networks (WSNs) are used interchangeably. In Section 3, we describe the smart-HOP mechanism and its main parameters, and illustrate some experimental results obtained in a controlled environment. The analytical and simulation models together with an extensive study of the impact of channel parameters are presented in Section 4. In Section 5, we provide the best parameter tuning based on an extensive experimental analysis in a realistic environment. Related work is outlined in Section 6. Finally, we conclude the paper and discuss our most relevant findings in Section 7.

2 PROBLEM STATEMENT

This section elaborates on the need to calibrate hand-offs according to the particular characteristics of low-power wireless networks and on the parameters that should be taken into account when designing a hand-off mechanism.

A naive solution to support mobility in WSNs is for mobile nodes (MNs) to broadcast messages to all access points (APs) in their vicinity. These broadcast approach, while simple, has a major limitation: broadcasts lead to redundant information at neighboring APs (since more than one AP may receive the same packet). This implies that the fixed infrastructure has to either waste resources in forwarding the same information to the end point, or to use a complex scheme, such as data fusion, to eliminate duplicated packets locally. A more efficient solution is for mobile nodes to select a single AP to transmit data at any given time. This alternative requires nodes to perform hand-offs between neighboring APs. Contrarily to more powerful wireless systems, such as cellular networks, which have typically advanced spread spectrum radios and high energy resources, WSNs have severely constrained resources. Hence, we need a better understanding of the hand-off process in low-power wireless networks.

Limitations of low-power links. Low-power links have two characteristics that affect the hand-off process: short coverage and high variability [15], [16]. Several empirical studies revealed the existence of three distinct reception regions in a wireless link; connected, transitional, and disconnected [17]. The transitional region is often quite significant in size, and is generally characterized by high variance in reception rates and asymmetric connectivity. In WSN applications, most of the links (more than 50% [15]) are in the transitional region.

Studies show that WSN links have high unreliability in dense deployments [18], [19]. The high variability of links has a direct impact on the stability of hand-offs. When not designed properly, hand-off mechanisms may degrade the network performance due to the *ping-pong* effect, which consists in mobile nodes having consecutive and redundant hand-offs between two APs due to sudden fluctuations of their link qualities. This usually happens when a mobile node moves in the vicinity of two APs. Hence, to effectively cope with link instability, a hand-off mechanism should calibrate the appropriate thresholds, taking into account the variance of the wireless links.

The transitional region for wireless nodes using the CC2420 radio transceiver encompasses the approximate range [-92 dBm, -80 dBm]. Intuition may dictate that the hand-off should be performed within the connected region as it indicates more reliable links. In practice, a hand-off should start when the link with the current (serving) AP drops below a given value (T_l) and should stop when it finds a new AP with the required link quality (above T_h).

Figure 1(a) depicts an example of inefficient hand-off and illustrates the negative impact of this conservative approach. In this scenario, the lower threshold is set to -85 dBm, and the upper threshold is set

¹The extended version of this paper is available online [14].

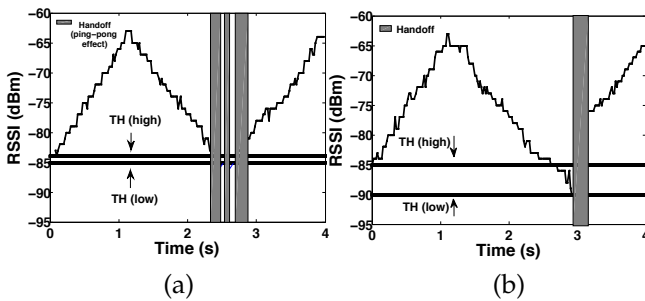


Fig. 1. (a) an example of inefficient hand-off with narrow *hysteresis margin* (1 dBm), $T_l = -86$ dBm and $T_h = -85$ dBm, resulting in three consecutive hand-offs (ping-pong effect). (b) an example of an efficient hand-off with wide *hysteresis margin* (5 dBm), $T_l = -90$ dBm and $T_h = -85$ dBm, resulting in a single hand-off [13].

to 1 dBm higher. This particular choice of parameters results in three undesirable consecutive hand-offs between the two contiguous APs (three shadowed vertical bars), which we refer to as *ping-pong effect* and that results in a long network inaccessibility time (700 ms). Increasing the threshold margin to 5 dBm (as illustrated in Figure 1(b)) eliminates the ping-pong effect (one shadowed vertical bar only) and hence reduces the hand-off delay to approximately 200 ms. This simple example shows that studying the low-power link characteristics is paramount for obtaining efficient hand-offs.

3 BASICS ON THE SMART-HOP

In this section, first we explain the data communication between the MN and a fixed infrastructure of APs, according to the smart-HOP procedure. Then, we highlight the importance of three parameters: *window size*, *hysteresis threshold* and *stability monitoring*. Afterward, we compare the cost of communication in smart-HOP with conventional hand-off approaches. Evaluation based on experiments in a controlled environment (model train moving in a square track) is then discussed.

3.1 The smart-HOP algorithm

The smart-HOP algorithm has been proposed in [13]. The algorithm has two main phases: (i) *Data Transmission Phase* and (ii) *Discovery Phase*. A timeline of the algorithm is depicted in Figure 2.

For the sake of clarity, let us assume that a node is in the *Data Transmission Phase*². In this phase, the mobile node is assumed to have a reliable link with an AP, defined as serving AP in Figure 2. The mobile node monitors the link quality by receiving *reply* packets from the serving AP. Upon receiving n data packets in a given window, the serving AP replies with the average RSSI or SNR of the n packets. If no packets are received, the AP takes no action. This may lead

²smart-HOP has a simple initialization phase that is similar to the *Discovery Phase*.

to disconnections, which are solved through the use of a time-out mechanism. It is important to notice that smart-HOP filters out asymmetric links implicitly by using reply packets at the Data Transmission and Discovery Phases. If a neighboring AP does not have active links in both directions, that AP is simply not part of the process. The smart-HOP process relies on three main parameters, follows.

Parameter 1: window size (ws). It represents the number of packets required to estimate the link quality over a specific time interval³. A small ws (high sampling frequency) provides detailed information about the link but increases the processing of reply packets, which leads to higher energy consumption and lower delivery rates. The packet delivery reduces as the MN opts for performing some unnecessary hand-offs. The hand-off is triggered by detecting low quality links, resulting from the decrease of the signal strength. On the other hand, a large ws (low sampling frequency) provides only coarse grained information about the link and decreases the responsiveness of the system, which is not suitable for mobile networks with dynamic link changes.

Parameter 2: hysteresis margin (HM). In WSNs, the selection of thresholds and *hysteresis margins* is dictated by the characteristics of the transitional region and the variability of the wireless link. The thresholds should be selected according to the boundaries of the transitional region. The transitional region is often quite significant in size and hence a large number of links in the network (higher than 50%) are unreliable [20], [21]. Therefore, wireless nodes are likely to spend most of the time in the transitional region.

A tight estimation of the threshold level within the transitional region is obtained from experimental analysis. If the T_l threshold is too high, the node could perform unnecessary hand-offs (by being too selective). If the threshold is too low, the node may use unreliable links. The *hysteresis margin* plays a central role in coping with the variability of low-power wireless links. If the *hysteresis margin* is too narrow, the mobile node may end up performing unnecessary and frequent hand-offs between two APs (ping-pong effect), as illustrated in Figure 1. If the *hysteresis margin* is too large, hand-offs may take too long, which ends up increasing the network inaccessibility times, and thus decreasing the delivery rate.

Parameter 3: stability monitoring (m). Due to the high variability of wireless links, the mobile node may detect an AP that is momentarily above T_h , but the link quality may decrease shortly after handing-off to that AP. In order to avoid this, it is important to assess the stability of the candidate AP. After detecting an AP with the link quality above T_h , the MN sends m further bursts of beacons to check the stability of that AP. The burst of beacons stands for the ws request beacons followed by the reply packets received from

³In the extended experiments, the beacons' interval increased from 5 ms (in the preliminary experiments) to 10 ms. The longer period in transmitting beacons increased the chance of beacon reception at the APs. In the *Data Transmission Phase*, after sending a burst of beacons, the MN waits for 10 ms to receive the reply from the serving parent. In the *Discovery Phase*, the waiting time is increased to 100 ms in order to get replies from all neighbor APs.

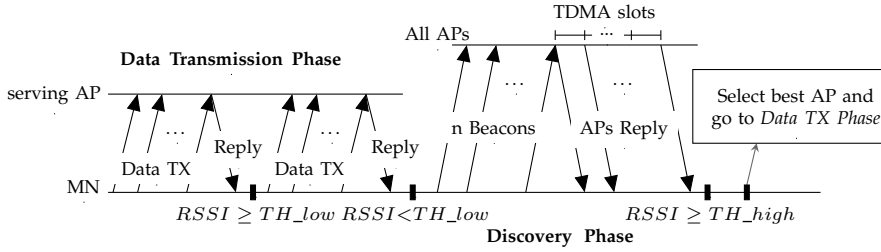


Fig. 2. Timing diagram of the smart-HOP mechanism [13].

the neighboring APs. As can be easily inferred, the *stability monitoring* and the *hysteresis margin* parameters are tightly coupled. A wide *hysteresis margin* requires a lower m , and vice-versa. In the experimental evaluation (Section 5), we will show that an appropriate tuning of the *hysteresis margin* will lead to $m = 1$.

3.2 Why smart-HOP for WSNs?

Hand-offs are used in all mobile wireless networks. This simple concept of switching from one AP to another requires very careful design considerations, so that the application requirements and system limitations are respected. In this subsection, first we outline the main features of hand-off processes in Cellular and WiFi networks, and show that a new approach is required for low-power wireless networks (smart-HOP), comparing the communication cost of these hand-off approaches.

In Cellular networks, the base stations have high energy, processing and communication resources. All the APs are connected through a stable wired backbone, which is responsible for making hand-off decisions. All mobile nodes periodically broadcast beacons along with their data packets. At the same time, the base stations communicate with each other and assess the location and the link quality of all mobile nodes. By detecting a low quality link, the base stations decide for the next servicing base station (for the MN).

In WiFi networks, power and bandwidth are more limited than in cellular networks. Thus, performing a centralized decision at the base stations (similar to cellular networks) is not efficient. In these networks, a distributed hand-off decision is performed at the MNs. All APs periodically broadcast beacons in various available channels with a precise timing (to eliminate overlapping). The MN periodically broadcasts request packets in all channels to get immediate replies (beacons) from neighbor APs. During the *Data Transmission Phase*, the MN gets periodic beacons from the serving AP. By detecting a low quality link with the serving AP and high quality link with one of the neighbors, the MN decides to trigger a hand-off process.

smart-HOP can reduce the communication overhead. Applying the aforementioned techniques in WSNs requires a lot of beaconing, which in turn increases the network overhead, collisions and energy consumption. In low-power low-cost wireless networks with a poor backbone of APs, a centralized

approach is not feasible. On the other hand, a periodic beaconing of APs in a single radio network leads to packet collisions. smart-HOP is a distributed hand-off mechanism where MNs are responsible for broadcasting beacons after detecting a low quality link.

Let us assume a simple terminology to depict the communication overhead of smart-HOP. Denoting C_{tx} , C_{rx} , C_b , and n_{AP} as the transmission cost, reception cost, beaconing cost and average number of APs available⁴. The communication overhead of all wireless networks is formulated as follows. (i) WSNs with smart-HOP is $(C_{tx} + C_{rx})(1 + \frac{1}{ws})$, (ii) WSNs with broadcast approach is $C_{tx} + n_{AP} \times C_{rx}$, (iii) WiFi networks is $(C_{tx} + C_{rx}) + (n_{AP} \times C_b + n_{AP} \times C_{rx})$, and (iv) cellular networks is $(C_{tx} + n_{AP} \times C_{rx}) + (C_b + n_{AP} \times C_{rx})$. It is important to note that in estimating the costs, we considered the general concept of hand-off that is common in most of the literature. Simple manipulations lead to the following conditions⁵.

- 1) $C_{\text{smart-HOP}} > C_{\text{Broadcast}}$
if $(ws \times n_{AP} - ws - 1)C_{rx} < C_{tx}$
- 2) $C_{\text{smart-HOP}} > C_{\text{cellular}}$
if $ws \times C_b + C_{rx}(2n_{AP} \times ws - ws - 1) < C_{tx}$
- 3) $C_{\text{smart-HOP}} > C_{\text{WiFi}}$
if $ws \times n_{AP} \times C_b + C_{rx}(n_{AP} \times ws - 1) < C_{tx}$

The only situation that verifies the above conditions is to have a very high transmission cost compared to the reception cost. In practice, transmission and reception costs for low-power radios such as the CC2420 radio are rather similar ($C_{tx} \cong C_b \cong 19$ mA and $C_{rx} \cong 24$ mA [22]). Hence, smart-HOP is expected to be more efficient than the broadcast approach in WSNs and the conventional hand-off approaches in other wireless networks. The cost of the four hand-off approaches is illustrated in Figure 3.

3.3 Test-bed setup for the preliminary experiments

The aim of the *preliminary experiments* was to investigate the feasibility of the smart-HOP mechanism in a controlled environment with limited dependencies on link dynamics. In this way, we deployed a model-train in a large room (7 m×7 m) and the

⁴The beaconing (process of transmitting beacons) is defined separately in order to be distinguished from the data transmission (C_{tx}). However, the cost of transmitting a data packet and a beacon is assumed equal.

⁵Two more conditions of $n_{AP} > 1$ (existence of more than one AP in the range of each MN) and $ws > 1$ (to apply a windowing process) are also respected.

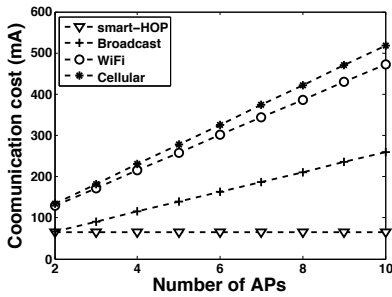


Fig. 3. The communication costs of broadcast in WSNs and the hand-off approaches in wireless networks.

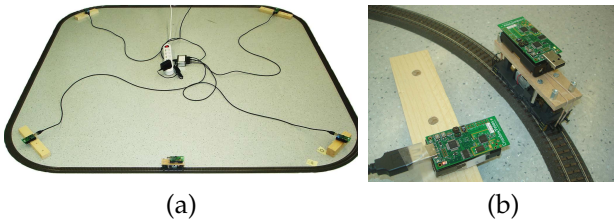


Fig. 4. smart-HOP of the preliminary experiments for assessing and tuning the smart-HOP hand-off mechanism (a) 4 APs and a MN, (b) MN passing by an AP [13].

locomotive followed a $3.5 \text{ m} \times 3.5 \text{ m}$ square layout (an extensive description on the *preliminary experiments* is presented in [13]). The speed of the locomotive was about 1 m/s (similar to the average human walking speed). Figure 4(a) depicts the experimental scenario and Figure 4(b) shows the locomotive passing by an AP. To prevent extreme deployment conditions such as very high or very low density of APs, we guaranteed a minimum overlap between neighboring APs. This was achieved by choosing a proper transmission power (-20 dBm) and locating the APs far enough from each other.

The transmission period of the beacon and data packets was 10 ms . This value is close to the maximum rate possible, considering the processing, propagation and communication delays. The idea behind choosing the maximum data rate was to evaluate smart-HOP for scenarios with more demanding QoS requirements. Four APs were located at the corners of the railway, and up to six additional APs were randomly placed, to assess the impact of AP's density.

We ran four laps with the MN broadcasting packets, in each set of experiments. The experiments were run at different times of the day, during several days and with a different number of people in the room. In all these scenarios, the mobile node required a minimum of four hand-offs per lap. The time of the day and number of people in the room (1 to 4) did not seem to affect the number of hand-offs. We utilized an interference-free channel to calibrate the parameters (channel 15, with a constant noise-floor of -94 dBm).

Performance metrics. In a mobile network, it is crucial to maintain network connectivity as much as possible by minimizing the inaccessibility periods and

the frequency of hand-offs. In this line, we define the following three metrics to evaluate the performance of the smart-HOP algorithm.

- 1) *Packet delivery ratio.* It defines the ratio of packets successfully delivered to the total number of packets sent.
- 2) *Number of hand-offs.* This metric helps identifying the existence of ping-pong effect. Multiple hand-offs in a single trip of a MN from one AP to another AP means that the ping-pong effect has occurred.
- 3) *Hand-off delay.* It represents the network inaccessibility time and is measured as the average time spent in the *Discovery Phase* (to find a better AP). Given that smart-HOP is a hard hand-off mechanism, nodes cannot send packets during this time; hence, this metric should be minimized.

3.4 Thresholds, hysteresis margin and AP stability

The first step in a hand-off scheme is to determine when should a node deem a link as weak and start looking for another AP (represented as T_l in our framework). In the sensor networks community, the *de-facto* way to classify links is to use the connected, transitional and disconnected regions.

An educated guess for the width of the *hysteresis margin* could be obtained from Figure 1 (based on the 10 dBm width of the transitional region). However, while this value would guarantee that *all* links above T_h are reliable, it would also increase the amount of beacons and time required to reach T_h . In order to evaluate this region extensively, we considered different values for each hand-off parameter, as shown in Table 1. For example, if we consider scenario *A* with a 5 dBm margin and stability 2, it means that after the mobile node detects an AP above $T_h = -90 \text{ dBm}$, the node will send two 3-beacon bursts to observe if the link remains above T_h . The *hysteresis margin* HM captures the sensitivity to the ping-pong effect, and the number of bursts m reflects the stability of the AP candidate (recall that each burst in m contains three beacons).

We conducted experiments for all the scenarios in Table 1. For each evaluation tuple $\langle T_l, HM, m \rangle$, the mobile node performed four laps, leading to a minimum of 16 hand-offs. In each trip from one AP to the next, an efficient scenario must perform one hand-off, which in turn leads to four hand-offs in one lap trip. The experiments provided some interesting results. First, we show the results for the narrow margin (1 dBm), and then the ones for the wider margin (5 dBm).

TABLE 1
Description of scenarios [13]

Scenarios	T_l	HM	m
A	-95 dBm	$1, 5 \text{ dBm}$	$1, 2, 3$
C	-85 dBm	$1, 5 \text{ dBm}$	$1, 2, 3$
B	-90 dBm	$1, 5 \text{ dBm}$	$1, 2, 3$
D	-80 dBm	$1, 5 \text{ dBm}$	$1, 2, 3$

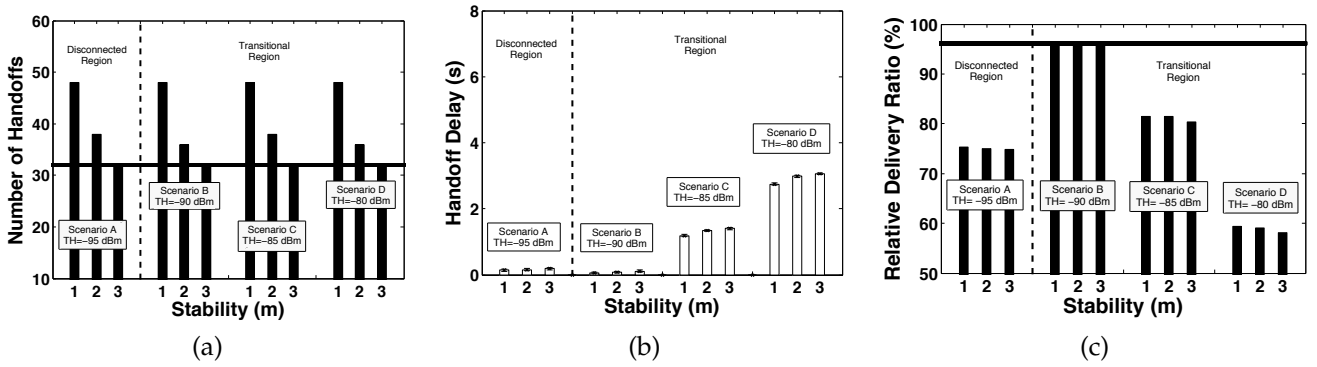


Fig. 5. Results for narrow *hysteresis margin* ($HM = 1dBm$). (a) number of hand-offs, (b) mean hand-off delay, (c) relative delivery ratio. The horizontal lines represent the results for the best scenario: 32 for the number of hand-offs and 96% for the relative delivery ratio [13].

3.5 Observations

The high variability of low-power links can cause severe ping-pong effect. Figure 5(a) depicts the total number of hand-offs for the narrow margin case. We observed two important trends. First, all scenarios exhibit ping-pong effect. The minimum number of hand-offs in this scenario is supposed to be 16 (one hand-off in each trip from one AP to another). However, the figure indicates 32 to 48 hand-offs in 4-laps trip. Due to the link variability, the transition between neighboring APs requires between 2 and 3 hand-offs. Second, a higher stability value m helps in alleviating the ping-pong effect. We observe that for all scenarios the higher the stability, the lower the number of hand-offs.

Thresholds at the higher end of the transitional region lead to longer delays and lower delivery rates. Figure 5(b) depicts the average hand-off delay for various thresholds T_l . A threshold selected at the higher end of the transitional region (-85 or -80 dBm, scenarios C and D) can lead to an order of magnitude more delay than a threshold at the lower end (-90 dBm, scenario B). This happens because mobile nodes with higher thresholds spend more time looking for overly reliable links (the *Discovery Phase* takes longer), and consequently less time transmitting data (lower delivery rate). Figure 5(c) depicts the relative delivery rate and captures this trend. In order to have a reference for the absolute delivery rate, we measured several broadcast scenarios considering a high transmission rate and a 4-access point deployment. We found that the average delivery rate was 98.2%, with a standard deviation of 8.7. This implies that there are limited segments with no coverage at all. Furthermore, the overlap is minimal, which tests the agility of the hand-off mechanism (as opposed to dense deployments, where very good links are abundant). Scenario A in Figure 5(c) is an exception, because the MN remains disconnected for some periods of time. As shown in Figure 4(a), no link goes below -95 dBm, hence, when this threshold is used, the *Discovery Phase* does not start because the link goes below T_l , but because disconnection time-outs occur.

The most efficient hand-offs seem to occur for thresholds at the lower end of the transitional region

and a *hysteresis margin* of 5 dBm. Figure 6 shows that scenario B (-90 dBm) with stability 1 maximizes the three metrics of interest. It leads to the lowest number of hand-offs, with the lowest average delay and highest delivery rate. It is important to highlight the trends achieved by the wider *hysteresis margin*. First, the ping-pong effect is eliminated in all scenarios of Figure 6(a). Second, contrarily to the narrower *hysteresis margin*, monitoring the stability of the new AP for longer periods ($m = 2$ or 3) does not provide any further gains, because the wider margin copes with most of the link variability.

4 ANALYTICAL MODEL AND EVALUATION

The performance of algorithms in low-power wireless networks may greatly change depending on the network layout and environmental conditions. We conceived an analytical model for further evaluating the smart-HOP algorithm. In this probabilistic analysis, we study the impact of two major channel parameters:

- 1) *path-loss exponent* (η). It measures the power of radio frequency signals relative to distance.
- 2) *standard deviation* (σ). It measures the standard deviation in RSSI measurements due to log-normal shadowing.

The values of η and σ change with the frequency of operation and the clutter and disturbance in the environment. At this stage, we study the smart-HOP performance in various environmental conditions to observe the feasibility and efficiency of the algorithm.

In this section, first we describe the system model and the probabilistic model for a hard hand-off process in WSNs. Then, we investigate the impact of channel parameters on the hand-off performance and check the analytical results through a simulation analysis. After confirming the viability of the algorithm, we will move to more realistic experiments for better tuning the relevant parameters (Section 5).

4.1 Probabilistic model

It is important to consider a “probabilistic” or “analytical” model that is faithful to the underlying physical model while being amenable to analysis. We assume a scenario consisting of two APs (AP_a and AP_b) and

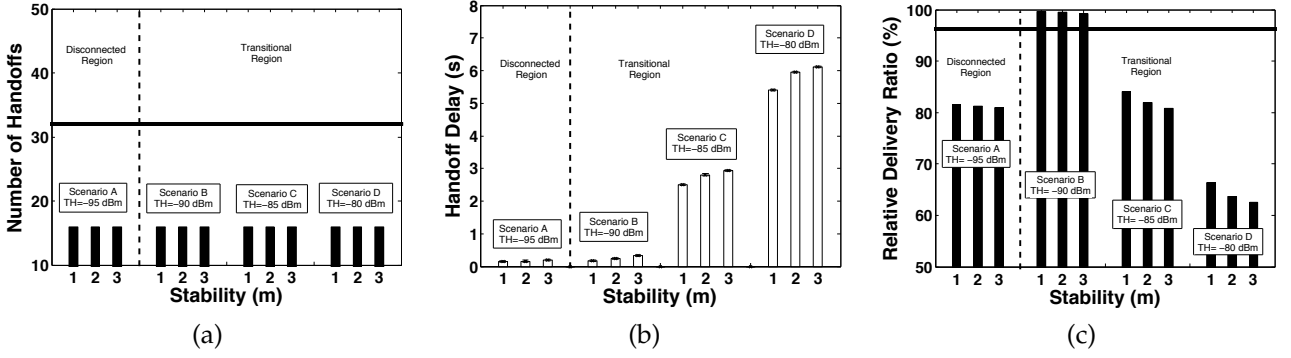


Fig. 6. Results for wide *hysteresis margin* (HM=5 dBm). (a) number of hand-offs, (b) mean hand-off delay, (c) relative delivery ratio. The horizontal lines represent the best results obtained for HM=1 dBm [13].

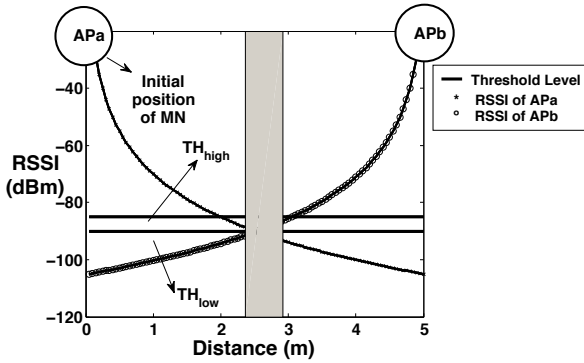


Fig. 7. System model. It show the RSSI fluctuations of AP_a and AP_b in a 10 m distance. The threshold levels are assumed -85 and -90 dBm. The hand-off happens in the middle of this trip (shadow area).

a MN. This assumption is enough without loss of generality, as we are considering a hard hand-off process. In the probabilistic model, we ignore the *window size* and *stability monitoring* by considering $ws=m=1$, as adding these parameters into the analysis increases the complexity of the equations and is not in the scope of our work.

The two main hand-off performance metrics are the probability of ping-pong effect and the expected hand-off delay. The system model and a general behavior of smart-HOP are shown in Figure 7. The two APs are separated by distance $d(m)$ while the MN moves from the vicinity of AP_a to the vicinity of AP_b along a straight line. In this model, the MN moves with a constant speed of 1 m/s. The received signal strength from AP_a declines till it reaches the lower threshold level T_l , thus triggering the hand-off process. From this point onwards, the MN stops communication with AP_a and tracks the RSSI of the neighboring AP, AP_b , (single radio eliminates the probability of collecting RSSI readings from multiple neighbor APs at the same time). If the mobile node observes a signal strength above a higher threshold level, T_h , the hand-off process is considered to be finished. The hand-off period is marked with a shadowed vertical bar in Figure 7.

Link quality monitoring. There are different ways

of measuring the link quality metric. In this work, we consider the RSSI as the link quality level. The probabilities of being below the lower threshold level and above the higher threshold level are defined by using a Q-function. In this turn, the traveling path of the MN is divided into a number of slots. For the sake of simplicity, we consider the same sampling rate for both the *Discovery* and *Data Transmission Phases*. These probabilities are expressed as follows.

$$P(R_a(i) < T_l) = Q\left(\frac{-T_l + R_a(i)}{\sigma}\right)$$

$$P(R_b(i) > T_h) = Q\left(\frac{T_h - R_b(i)}{\sigma}\right)$$

Where $Q(\cdot)$ is the complementary distribution function of the standard Gaussian, i.e., $Q(x) = \int_x^\infty (1/\sqrt{2\pi})e^{-t^2/2}dt$, $R_a(i)$ and $R_b(i)$ indicates the RSSI values from AP_a and AP_b at slot i , and σ (in dB) expresses the standard deviation.

Radio channel model. The received signal strength is estimated by a log-normal shadowing path-loss. According to this model, $R(i)$ (in dBm) (RSSI level at a given slot i) from the transmitter is given by [23]:

$$R(i) = P_t - \overline{PL}(d_0) - 10n \log_{10}(i/d_0) - X_\sigma \quad (1)$$

Where i corresponds to distance, P_t is the transmission power, $\overline{PL}(d_0)$ is the measured path-loss at reference distance d_0 , n is the path-loss exponent, and $X_\sigma = N(0, \sigma)$ is a Normal variable (in dB). The term X_σ models the path-loss variation across all locations at distance i from the source due to shadowing, a term that encompasses signal strength variations due to the characteristics of the environment (i.e., occlusions, reflections, etc.).

Smart-HOP probabilistic model. To evaluate the performance metrics, we define the possibility of starting and ending a hand-off process at each slot. As explained earlier, in WSNs with hard hand-off, the MN communicates with a single AP at each time-slot. The MN is initially connected to AP_a —see Figure 7. When the MN is traveling from AP_a to AP_b , it tracks the likelihood of the RSSI going below a threshold level, T_l , at each sampling interval. By observing a low quality link, the hand-off process starts. The probability of starting a hand-off at slot $s \in [1, k]$ is defined as follows (k indicates the total number of

slots).

$$P(S(s)) = \left[\prod_{i=1}^{s-1} P(R_a(i) \geq T_l) \right] \times P(R_a(s) < T_l) \quad (2)$$

The first part of the equation indicates the observation of a number of slots ($s-1$) with good/acceptable link quality level (above T_l). The second part denotes the observation of the low link quality for the first time (below T_l). The following settings are used in all future evaluations across this section: $\sigma = 4$ dB, $\eta = 4$, $P_t = 0$ dBm, $d_0 = 1$ m, $d = 5$ m, $PL(d_0) = -55$ dB, $ws = m = 1$, $T_l = -90$ dBm and $T_h = -85$ dBm. The network related values are set according to the most efficient scenario of the *preliminary experiments*.

By starting the hand-off process at slot/location s , the MN disconnects from the corresponding AP that was servicing the MN. At this moment, the MN starts assessing the other neighboring AP to choose the one with higher threshold level ($RSSI > T_h$). The hand-off finishes when the MN observes a high link quality. Equation 6 formulates the probability of ending a hand-off at slot e considering the fact that the hand-off would have been started at slot s and the MN was disconnected from either AP_a or AP_b .

$$P(E(e) | S(s)) = \left[\prod_{i=s+1}^{e-1} (P(R_a(i) < T_h) \times P(R_b(i) < T_h)) \right] \times [1 - (P(R_a(e) < T_h) \times P(R_b(e) < T_h))] \quad (3)$$

This equation assumes that the hand-off occurs at slot s . The ending moment at slot $e \in (s+1, k]$ happens at a later stage by comparing the RSSI level of the APs to a higher threshold level, T_h . Hence, in practice it is a conditional probability and depends on a situation that has taken place previously at slot s .

The time span between the starting slot and the ending slot is called hand-off delay. It is possible to calculate the hand-off delay for all possible hand-offs starting at any slot. By considering each point as a starting moment of a hand-off process, we characterize the ending moments by the probabilities defined in Equation 6. The expected hand-off delay is computed by getting the weighted sum of all possible hand-off periods. It is defined as the product of the time spent in each possible hand-off process started at slot s and ended at slot e by the correspondent probabilities of starting a hand-off at slot s , $P(S(s))$, and ending it at slot e , $P(E(e) | S(s))$. For each hand-off starting at slot s , the hand-off would end at one of the slots from $s+1$ to k . The sum of all these possible situations defines the expected delay for a hand-off started at a specific slot s . The overall expected hand-off delay is defined as follows.

$$Delay(s, e) = \sum_{s=1}^{k-1} \sum_{e=s+1}^k ((e-s) \times P(E(e) | S(s)) \times P(S(s))) \quad (4)$$

In order to measure the ping-pong effect in smart-HOP, a new term is defined that is called probability of restarting a hand-off. This situation happens when

a MN performs hand-off at an improper moment, thus leading to an unnecessary hand-off. The restarting of a hand-off always occurs after successfully ending the first hand-off at slot $r \in (2, k]$. This means that the probability of restarting is also a conditional probability that depends on ending a hand-off at an earlier stage. Since the MN may have been connected to either AP_a or AP_b , the signal strength should be evaluated for both cases. The equation is defined as follows.

$$P(R(r) | E(e)) = \left[\prod_{i=e+1}^{r-1} (1 - P(R_a(i) < T_l) \times P(R_b(i) < T_l)) \right] \times [P(R_a(r) < T_l) \times P(R_b(r) < T_l)] \quad (5)$$

The second disconnection of the MN in this trip will be ended at slot p , which is defined in the following equation.

$$P(P(p) | R(r)) = \left[\prod_{i=r+1}^{p-1} (P(R_a(i) < T_h) \times P(R_b(i) < T_h)) \right] \times [1 - (P(R_a(p) < T_h) \times P(R_b(p) < T_h))] \quad (6)$$

To find out the probability of ping-pong effect, the full history of a MN since the first start of hand-off to the end and restarting again are taken into account. Equation 7 illustrates the cases that lead to a ping-pong effect at slot p , as follows.

$$P(P(p)) = \left[\left(\prod_{i=1}^{s-1} P(R_a(i) < T_l) \right) \times P(R_a(s) < T_l) \right] \times \left[\prod_{i=s+1}^{e-1} (P(R_a(i) < T_h) \times P(R_b(i) < T_h)) \right] \times [1 - P(R_a(e) < T_h) \times P(R_b(e) < T_h)] \times \left[\prod_{i=e+1}^{r-1} (1 - P(R_a(i) < T_l) \times P(R_b(i) < T_l)) \right] \times [P(R_a(r) < T_l) \times P(R_b(r) < T_l)] \times \left[\prod_{i=r+1}^{p-1} (P(R_a(i) < T_h) \times P(R_b(i) < T_h)) \right] \times [1 - P(R_a(p) < T_h) \times P(R_b(p) < T_h)] \quad (7)$$

To find out the total probability of ping-pong effect, we define the following equation in a more abstract way. For each case of hand-off occurrence at slot $s \in (0, k-2]$, there is a chance to finish the hand-off at one of the upcoming slots $e \in (s, k-1]$. Similarly for each e , as an ending slot, there is a chance of restarting another hand-off at slot $r \in (e, k]$.

$$\begin{aligned} \text{Total probability of ping-pong} = & \sum_s^{k-3} \sum_e^{k-2} \sum_r^{k-1} \sum_p^k P(S(s)) \times P(E(e) | S(s)) \\ & \times P(R(r) | E(e)) \times P(P(p) | R(r)) \end{aligned} \quad (8)$$

Performance metrics. To evaluate the performance of the smart-HOP mechanism, two main metrics are considered, which are derived from the above equations.

- 1) *probability of ping-pong effect*. It shows the probability of reconnecting to AP_a after the first hand-off from AP_a to AP_b . This situation happens after observing a low quality link $R_b(i) < T_l$ at AP_b at slot i , where there was a high quality link $R_b(i-1) > T_l$ at slot $i-1$.
- 2) *expected hand-off delay*. It indicates the expected hand-off delay for each possible starting point of hand-off from AP_a to AP_b .

In the following subsections, we study the impact of some parameters, which were either neglected or not feasible to address due to the network limitations in the *preliminary experiments*.

4.2 Impact of channel parameters

An increase in the path-loss exponent leads to longer hand-off delay and higher probability of ping-pong effect. The path-loss exponent varies depending on the environmental conditions. The path-loss parameter may be less dynamic in some applications with stationary nodes and static environments or oppositely may be highly variable in some other situations like mobile WSN applications [24]. Figure 8(a) illustrates the variation of the RSSI at AP_a while the MN is moving toward AP_b . The larger the path-loss exponent is, the higher the slope of the RSSI decrease will be. In smart-HOP design, we aim at choosing a hand-off starting level below the intersection of the received signal power from AP_a and AP_b . This will reduce the chance of ping-pong effect. The ending level is supposed to be at this intersection or slightly higher. In practice, it is recommended to pick a higher level for ending point, to cancel out sudden fluctuations of the RSSI.

An increase in the shadowing variance enlarges the transitional region, which in turn causes higher link unreliability and ping-pong effect. This channel parameter describes the received signal strength fluctuation caused by flat fading. By increasing σ , the probability of entering the transitional region at closer distances from the transmitter and leaving it at farther distances increases; this results in a larger transitional region —see Figure 8(b) [20].

By enlarging the channel parameters, the hand-off delay increases. Figure 9 depicts a matrix, with the x-axis representing the path-loss exponent and the y-axis representing the shadow-fading. We observe an increasing trend in the hand-off delay in each row and column when increasing each channel parameter. A larger path-loss exponent causes faster RSSI decrease. Hence, the MN enters the hand-off process at earlier stages. Finding a high link quality is postponed to later stages, which in turn increases the hand-off delay. Larger shadow-fading increases the RSSI standard deviation, which expands the transitional region. Therefore, any disconnection from the point of attachment requires a longer time assessing the wireless link to detect a high quality link in the transitional region.

By enlarging the channel parameters, the probability of ping-pong effect increases. Figure 10 shows that increasing any channel parameter causes higher

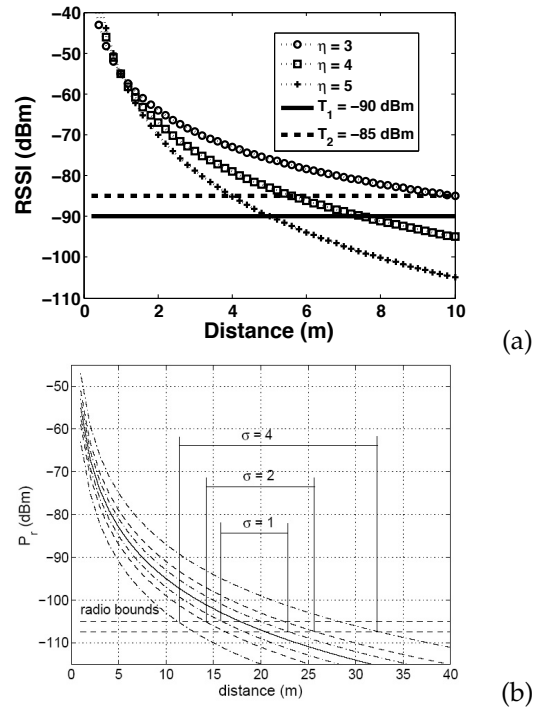


Fig. 8. Impact of channel parameters on the RSSI with $T_l = -90$ dBm and $HM = 5$ dBm, (a) impact of path-loss exponent on RSSI, and (b) impact of shadow fading on the RSSI [20].

Channel Parameters	$\eta=1$	$\eta=2$	$\eta=3$	$\eta=4$	$\eta=5$	$\eta=6$
$\sigma=1$	8.2e-099	1.4e-045	2.4e-014	0.0216	0.0387	0.0469
$\sigma=2$	3.1e-027	9.1e-014	2.5e-005	0.0324	0.0408	0.0470
$\sigma=3$	2.4e-013	2.8e-007	0.0022	0.0371	0.0422	0.0477
$\sigma=4$	2.6e-008	7.5e-005	0.0109	0.0398	0.0433	0.0496
$\sigma=5$	6.9e-006	0.0012	0.0215	0.0415	0.0443	0.0519
$\sigma=6$	1.6e-004	0.0054	0.0297	0.0428	0.0453	0.0537

Fig. 9. Impact of channel parameters on the overall expected hand-off delay in seconds (sampling rate of every 50 ms).

link variability, unreliability and instability. This is the main reason for noticing higher probability of ping-pong effect when increasing either the path-loss exponent or shadow fading parameters.

Studying the channel parameters (σ, η) reveals the high dependency of the hand-off process on environmental changes. However, these values do not fluctuate significantly in indoor environments [20]. In an efficient hand-off, the MN should perform the process within at most a single sample (50 ms in this example). Figure 9 shows an acceptable hand-off delay for most cases except with $\eta = 6$ and $\sigma > 4$. This condition rarely happens in outdoor environments [20]. Thus, we get to the conclusion that **smart-HOP is suitable for all environments, although for outdoor environments a user should perform a radio survey⁶ to obtain a better insight.**

⁶It is difficult to predict the values of channel parameters during an experiment. A radio survey is a process that determines the channel values before performing an experiment.

Channel Parameters	$\eta=1$	$\eta=2$	$\eta=3$	$\eta=4$	$\eta=5$	$\eta=6$
$\sigma=1$	0	0	1.8e-229	6.4e-144	5.4e-079	2.1e-034
$\sigma=2$	5.7e-120	3.7e-087	5.3e-060	1.7e-038	6.6e-022	2.2e-010
$\sigma=3$	1.0e-054	4.2e-040	5.7e-028	2.7e-018	1.0e-010	2.4e-005
$\sigma=4$	1.6e-031	2.7e-023	1.7e-016	6.8e-011	1.6e-006	0.0018
$\sigma=5$	1.4e-020	2.6e-015	5.5e-011	2.7e-007	1.7e-004	0.0128
$\sigma=6$	1.7e-014	7.2e-011	7.3e-008	2.8e-005	0.0022	0.0345

Fig. 10. Impact of channel parameters on the probability of ping-pong effect (sampling rate of 20 Hz).

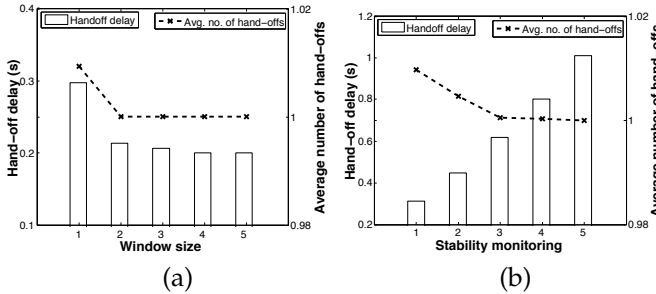


Fig. 11. Simulation analysis; (a) impact of window size in the *Data Transmission Phase*, and (b) impact of stability monitoring.

4.3 Simulation model

We performed a simulation study with MATLAB to verify the correctness of the probabilistic model [25]. In this model, we generated random values of RSSI at various distances from the serving AP and the neighboring AP with Equation 1. The mobile node started and ended the *Discovery Phase* by reading the RSSI values at each sampling slot. Studying the impact of network and channel parameters (T_i , HM , m , η and σ), we observed similar results to the ones from the probabilistic model. In the simulation model, we are able to consider higher values of ws and m . These parameters were ignored in the probabilistic model, for simplicity. We assume that the MN is initially connected to AP_a . By considering a sliding window ws and low threshold level T_i for starting a hand-off, the MN decides for the hand-off starting slot. Then by having the RSSI value of AP_b , and considering the stability parameter m , the MN decides for ending the hand-off. This process repeats for 10,000 trips and the results are averaged at the end of the simulation.

Impact of window size. This parameter is used in both the *Discovery Phase* and the *Data Transmission Phase*. In the preliminary experiments, we simply assumed $ws=3$ for both phases. In this simulation, we study the impact of *window size* in each phase separately.

Impact of window size in the Data Transmission Phase. By setting $ws=3$ for the *Discovery Phase* and varying it from 1 to 5 in the *Data Transmission Phase*, we get a decreasing trend of hand-off delay for the first 3 cases and then it remains unchanged —see Figure 11(a). This happens to the number of hand-offs as well. This means that a small *window size* value during the normal data communication of the MN, reduces the hand-off delay and the number of unnecessary hand-offs.

Impact of window size in the Discovery Phase. Increasing the number of beacons for assessing the neighboring APs requires more time, which is proportional to the sampling frequency. This case is somehow similar to the stability parameter that increases the period of link assessment. It is apparent that considering a few samples can compensate the fluctuations of random RSSI values. Hence, it is not logical to assume a large *window size* value for the *Discovery Phase* due to its negative impact on the hand-off delay. In the current model with 2 APs, the result is similar to the case when changing the stability parameter, thus it is not shown here. In case of higher density scenarios the results are different, but still the trend is equal.

Impact of stability monitoring. Increasing the *stability monitoring* reduces the link variability. Each unit of *stability monitoring* adds a new *Discovery Phase*, which is composed of a set of beacons and reply packets. The results in Figure 11(b) indicate that the hand-off delay has an increasing trend with a high slope, which is more steep than the case of increasing *window size* during the *Discovery Phase*. Considering the ping-pong effect, there is an improvement with a small stability parameter. In practice, we can substitute the stability parameter with the *window size* of the *Discovery Phase*. By this action, we can (i) reduce the link variability to eliminate the ping-pong effect and (ii) compensate the RSSI fluctuations to take accurate hand-off decisions. More insight into the simulation is provided in [14].

5 EXPERIMENTAL EVALUATION

The *preliminary experiments* [13] revealed the best thresholds for a hand-off process in a controlled environment. The probabilistic analysis proved that, in theory, smart-HOP is able to perform efficient hand-offs. At this stage, we set further experiments to enable a deeper analysis and fine-tuning of the algorithm in a more realistic environment.

We deployed a maximum of 6 APs with a minimum power level of -25 dBm in a 80 m^2 room. The APs were attached to walls at 1.5 m height from the ground (to guarantee a better connectivity). Figure 12 illustrates the position of each AP, furniture, walls and windows. A person was holding the mobile node and the logging PC⁷.

5.1 Test-bed setup

As we mentioned earlier, the two parameters of low threshold level and *hysteresis margin* are very important. Instead of starting the experiment with all the 6 APs, we first confine the scenario to 2 APs (AP_1 and AP_2 in Figure 12) and attached the MN to the person's shoulder, which faces the anchors in each trip from AP_1 to AP_2 . On the way back, the body eliminates the Line-of-Sight (LoS) communication. We

⁷At the beginning, we connected all APs to one laptop with passive USB cables and USB2.0 hubs. Then we observed some data loss during data transfer through the UART port. Adding more PCs did not solve the problem completely. Hence, we managed to get the data log from the MN with the cost of a person carrying a laptop during the experiment.

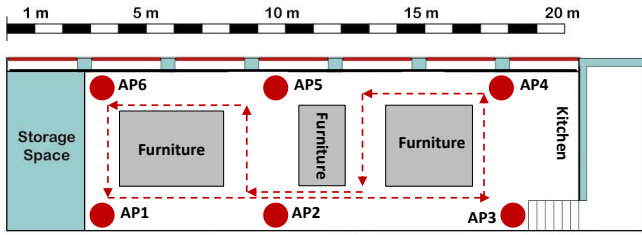


Fig. 12. The APs' deployment in a large room.

refer to this set of tests as *baseline experiments*. Less APs guarantees that there is no overlapping between neighboring APs. The person walks 4 times between these APs with a normal human walking speed (about 1 m/s).

The experimental area is a lab with at most 10 people sitting and three to five people moving randomly in all locations. The tests were performed on channel 15 of the CC2420 radio, which maybe affected by different sources of interference in the 2.4 GHz band (such as WiFi, Bluetooth and microwave devices). In order to obtain a better understanding of the frequency activities, we measured the 2.4 GHz spectrum usage; a WiFi-Spy spectrum analyzer verified that there was very low interference from other RF sources.

We evaluate smart-HOP in this realistic environment in two steps; (i) *baseline experiments* using 2 APs, to further analyze the lower threshold level and the *hysteresis margin* and (ii) *extended experiments* using 6 APs, to study the impact of *stability monitoring* and *window size*. In all tests, we employ SNR-based smart-HOP as it encompasses the interference in the environment.

5.2 Evaluation - baseline experiments

In the *preliminary experiments* (see Section 3), we considered four groups of lower threshold level (-95, -90, -85 and -80 dBm) with 2 values of *hysteresis margin* 1 and 5 dBm. The results indicated that -95 dBm is not a choice as the MN enters in the disconnected region. Now, we consider a wider range of lower threshold levels [-76, -90 dBm] increasing in 2 dBm steps, and higher threshold levels in the range of [-75,-89 dBm], which in turn generate *hysteresis margin* ranging from 1 to 15 dBm. All the 8 cases of lower threshold levels with variations of HM lead to 36 combinations. We compare all these situations in terms of number of hand-offs, hand-off delay and packet delivery ratio, walking four times between APs (AP_a and AP_b). The main goal at this stage is to pick situations that are more likely to be efficient and then reassess them with 6 APs, for further comparison. We observe the following facts.

- 1) Selecting the lower threshold level from the lower end of the transitional region with a wider *hysteresis margin* eliminates the ping-pong effect.
- 2) Either very wide *hysteresis margin* or narrow margin with large threshold level causes huge hand-off delay. A wide *hysteresis margin* obliges the MN to stay at the *Discovery Phase* for longer

periods of time. A narrow *hysteresis margin* with large value of lower threshold level causes an excessive number of hand-offs that eventually enlarges the hand-off delay.

- 3) A lower hand-off delay causes higher packet delivery ratio. The evaluations revealed that (i) increasing the *hysteresis margin* in all cases reduces the link variability and increases the packet delivery ratio, and (ii) higher values of packet delivery are achieved in situations with lower hand-off delay. The more efficient scenarios are noticed with *HM* between 3 and 7 dBm and T_l in the range of -86 to -90 dBm.

The most efficient scenarios in the *baseline experiments* are more elaborated in the *extended experiments*. The *baseline experiments* reveal that with the smallest T_l , -90 dBm, and $HM=5-7$ dBm, the hand-off delay is minimum, while obtaining a maximum delivery of packets. An educated solution is to keep the MN connected to the current link as much as possible, similarly to the *preliminary experiments*. Thus, we keep the same threshold level for starting the hand-off ($T_l=-90$ dBm) and compare the results of various *HM* values (3 to 8 dBm).

5.3 Evaluation - extended experiments

To find the best setting for the *hysteresis margin*, we increase the number of APs to six. Adding more APs creates a more realistic environment in which the mobile node experiences links overlapping. For each set of experiments, according to the selected *hysteresis margin*, the person walks in the room while the mobile node sends data periodically (every 100 ms). The person starts walking from AP_1 , along the dashed line shown in Figure 12. In some parts of the way, there are obstacles that prevent Line of Sight (LoS) communication. Moreover, random movement of people creates more dynamics in the environment. For each set of experiments, the person walked for about 15 minutes (transmitting 10,000 packets), which is about 15 full laps (dashed line circuit). At the end, we computed the average hand-off delay and the packet delivery ratio.

Increasing the *hysteresis margin* enlarges the hand-off delay as it forces the MN to attach to a higher link quality AP. Figure 13(a) shows that the hand-off delay is minimum with 3-5 dBm *hysteresis margin* and then it records a gradual increase. The reason is that by enlarging the margin, the chance of staying in the *Discovery Phase* for more than "one period" is higher. The one period stands for the case where after sending a burst of beacons and receiving reply packets, the MN is able to observe a good link to make the hand-off. The packet delivery ratio in Figure 13(b) illustrates a higher packet delivery ratio with $HM=5$ and 6 dBm. The packet delivery decreases with HM since there are unnecessary hand-offs. The higher HM causes fewer packets delivered as the MN stays in the *Discovery Phase* longer.

The *hysteresis margin* should be tuned to achieve an optimal trade-off between the delivery rate and delay. By choosing the lower end of the transitional

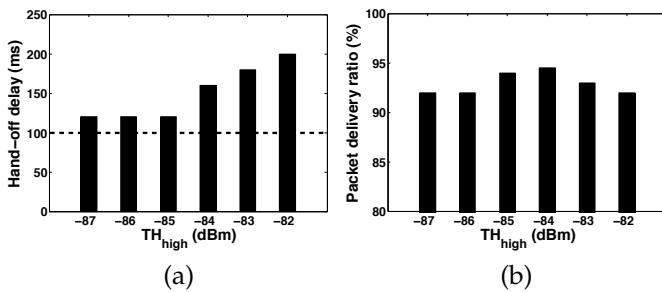


Fig. 13. More extensive experimental evaluation with 6 APs by considering $T_i = -90$ dBm, (a) average hand-off delay. The horizontal line shows the optimum hand-off delay computed by the analytical model. (b) absolute packet delivery ratio.

region (-90 dBm) as the threshold level, the *hysteresis margin* of 5 dBm is the best choice. The *stability monitoring* and the *window size* parameters are the two other important parameters, which are studied in these experiments.

Increasing the *stability monitoring* increases the hand-off delay. Increasing the *stability monitoring* has a direct impact on the hand-off delay—see Figure 14(a). Adding one unit to the stability requires observing a high quality link for one more sliding window. It is interesting to notice that this raise does not have a good impact on the packet delivery since we are shrinking the *Data Transmission Phase*. Considering the fact that a slight change in stability increases the hand-off delay significantly, it is wise to tune other related parameters with less impact. Thus, we opt for choosing the minimum stability value for the experiment and play with other parameters.

The *window size* parameter compensates the dynamics of the link. It should neither be too small nor too large as depicted in Figure 14(b). This parameter compensates the link variability and sudden RSSI changes. In a controlled environment, $ws=3$ was selected, according to the suggestions from related work. However, in a realistic scenario, there are more sources of disturbance: (i) there is a natural variation in human gait. When a movement experiment is repeated, a person carrying a node may move a bit faster or slower than before, or may deviate slightly from the previous path. Hence, a node may detect different signal strength at the same position [26]. (ii) The human body partly absorbs electromagnetic radiation, and the amount of absorbed energy depends—among other things—on the person’s physique and pose, and the radio frequency [27]. The results indicate that, in a real environment, a slightly higher window size, $ws=4$, increases the accuracy in terms of hand-off decision on exact moments. But enlarging more than this value does not improve the performance since it provides coarse grain information of the link. Considering wider window sizes reduces the responsiveness of the hand-off process.

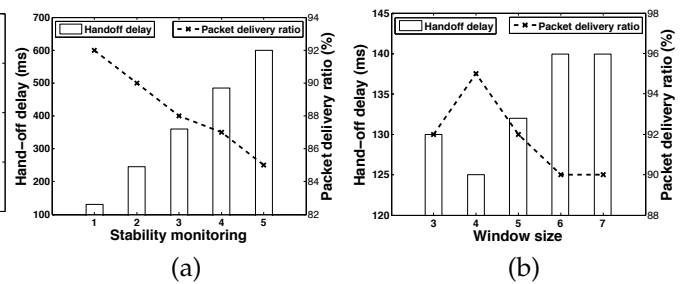


Fig. 14. (a) Impact of *stability monitoring*, (b) impact of *window size*.

6 BACKGROUND AND RELATED WORK

Hand-off mechanisms have been widely studied in cellular [28]–[30] and wireless local area networks [31]–[33], but did not receive the same level of attention in low-power wireless networks. There are two major strategies for the hand-off process: soft hand-off (network layer) and hard hand-off (MAC sub-layer). The soft hand-off requires lots of packet exchanges, thus impacting the sustainability of energy-constrained nodes. In any case, we address some of the latest algorithms using soft hand-off in WSNs [34], [35] as follows.

In [34], the authors focus on the hand-off in networks with mobile sensors and gateways. The mobile node is supposed to be in the range of multiple gateways that are periodically broadcasting router advertisement (RA) packets. Advertising their presence, enables the mobile node to decide for the best gateway. The connectivity of the network relies on the RA packets frequency; high frequency leads to network congestion while low frequency leads to low responsiveness of the network (thus to longer network inaccessibility).

A soft hand-off within 6LowPAN is proposed in [35]. The paper claims zero hand-off time and zero packet losses. The process is similar to [34]. However, it takes advantage of using two additional control messages, namely *Join* and *Join Ack* that are sent/received when the MN is still attached to the serving AP. This algorithm requires a huge amount of control message exchanges, increasing the probability of network congestion. Moreover, the zero hand-off delay was observed in a low sampling rate scenario, which may not be the case in many applications.

A more reasonable approach for low-power wireless networks (hard hand-off) is based on data link layer solutions [9], [13]. The respective authors claim that their approaches are adequate for passive decision with non-real-time support in [9] or for active decision with real-time support in [13].

In [9], the authors describe a wireless clinical monitoring system collecting vital signs from patients. In this study, the mobile node connects to a fixed AP by listening to beacons periodically broadcast by all APs. The node connects to the AP with the highest RSSI. The scheme is simple and reliable for low traffic data rates. However, there is a high utilization of bandwidth due to periodic broadcasts (similar to soft hand-offs) and hand-offs are passively performed whenever

the mobile node cannot deliver data packets.

We proposed a more reliable and faster hand-off approach for WSNs [13]. In this algorithm, hand-off is initiated at the mobile node, opposed to other algorithms in the literature. The MN keeps track of the link quality level during the *Data Transmission Phase*. A timer is responsible to detect the unreachability of the serving AP. Hence, the MN is able to detect the link degradation and unreachability of the serving AP within a short time. Then, the MN spends a time window assessing the neighboring APs to change to the best one.

The link quality is one of the parameters that significantly affects the hand-off performance. Different link quality estimators have been proposed for sensor networks. They apply different criteria to estimate the link status, such as RSSI, SNR, LQI or link asymmetry [36], [37]. In our case, due to the dynamics imposed by mobility, we use a simple and fast sampling of RSSI and SNR, which have been shown to provide reliable metrics [15].

7 CONCLUDING REMARKS

To the best of our knowledge, we are the first to systematically and empirically evaluate the hand-off in low-power wireless networks. We believe that this is important, because a panoply of WSN applications may require mobile nodes to report information reliably and in real-time, such as in clinical health monitoring and industrial automation. We proposed a reliable hand-off procedure that we dubbed as smart-HOP [13]. This hand-off scheme enables the MN to deliver data through the neighboring AP that offers the best link quality. In this line, some key parameters have a more significant impact on the performance of the hand-off. Experimental results in a controlled environment revealed the best threshold level ($T_l = -90$ dBm), *hysteresis margin* ($HM = 5$ dBm) and *stability monitoring* ($m = 1$) values, achieving hand-off delays of few tens of milliseconds and relative packet delivery ratios of around 98%.

It is well known that the performance of a low-power wireless system is very prone to environmental conditions. Thus, we conceived a probabilistic model to investigate the impact of the most relevant channel parameters on the hand-off process. We showed that the environmental changes have a direct impact on the smart-HOP performance, but it ends up performing well in various channel conditions. To have a better knowledge of the smart-HOP performance, it is recommended to perform a radio survey (to determine the path-loss exponent and shadowing standard deviation values) before the experiment. A simulation model was also designed to verify the probabilistic model. We studied the impact of network and channel parameters, confirming the correctness of the probabilistic analysis. The impact of *window size* and the *stability monitoring* parameters were also investigated. It was revealed that the *stability monitoring* has much more strength than the *hysteresis margin* in what concerns the hand-off delay.

We performed an extensive set of experiments in a more realistic environment. These were performed

in a large room with more people around, while the MN was attached to the shoulder of a person and (two to six) access points were attached to walls. A wider range of parameters was considered for the performance analysis (T_l from -90 to -76 dB, HM from 1 to 15 dBm, m from 1 to 5 and w_s from 3 to 7). We obtained similar parameter settings as in the preliminary experiments (in a controlled environment), which confirmed the stability of the smart-HOP mechanism in various environmental conditions and for several network scenarios.

The smart-HOP design shows some advantages but also limitations. It enables fast and reliable mobility support in low-power networks. It requires a number of stationary APs that are deployed in such a way to provide minimum overlap. In a dense deployment, the MN is very likely in the connected region of one AP, (which rarely happens in WSN applications). smart-HOP is inefficient for dense deployments as it is tuned based on the assumption of existing transitional regions. Moreover, the single radio characteristic limits the number of MNs that can be serviced at each AP. In cellular networks, each base station supports hundreds of MNs. The 802.15.4 radio allows one communication at each instance of time that limits the number of MNs.

This paper described the design and implementation of smart-HOP in a "protocol-agnostic way" with one MN and a number of APs. A future direction of this work is to support the smart-HOP within standard protocols and commercial off-the-shelf technologies (e.g. 6LoWPAN).

ACKNOWLEDGMENTS

The authors thank Patrick Meumeu Yonsi for his great help in revising the analytical model. This work was partially supported by National Funds through FCT (Portuguese Foundation for Science and Technology) and by ERDF (European Regional Development Fund) through COMPETE (Operational Programme 'Thematic Factors of Competitiveness'), within projects FCOMP-01-0124-FEDER-037281 (CISTER), FCOMP-01-0124-FEDER-014922 (MASQOTS); also by FCT and the EU ARTEMIS JU funding within ARROWHEAD project, ref. ARTEMIS/0001/2012, JU grant 332987.

REFERENCES

- [1] (2013) Final report from the nsf workshop on future directions in wireless networking. [Online]. Available: <http://ecedha.org/docs/nsf-nets/final-report.pdf?sfvrsn=0>
- [2] (2013) European commission, "factories of the future 2020: multi-annual roadmap for the contractual ppp under horizon 2020", research roadmap produced by the european factories of the future research association (effra). [Online]. Available: <http://www.effra.eu/attachments/article/129/Factories%20of%20the%20Future%202020%20Roadmap.pdf>
- [3] P. J. Marron, D. Minder, and S. Karnouskos, *The Emerging Domain of Cooperating Objects*. Springer, 2012.
- [4] (2012) Ginseng: performance control in wireless sensor networks. [Online]. Available: <http://www.ucc.ie/en/misl/research/previous/ginseng/>
- [5] (2009) Fasys: Absolutely safe and healthy factory. [Online]. Available: <http://www.fasys.es/en/proyecto.php>
- [6] (2010) flexware : Flexible wireless automation in real-time environments. [Online]. Available: <http://www.flexware.at/>

- [7] J. Martinez-de Dios, A. Jimenez-Gonzalez, A. San Bernabe, and A. Ollero, "Conet integrated testbed architecture," in *A Remote Integrated Testbed for Cooperating Objects*, ser. SpringerBriefs in Electrical and Computer Engineering. Springer International Publishing, 2014, pp. 23–39. This work has been carried out within the Cooperating Objects European Network of Excellence <http://www.cooperating-objects.eu/>.
- [8] R. Silva, J. Silva, and F. Boavida, "A proposal for proxy-based mobility in wsns," *Computer Communications*, 35(10), 2012.
- [9] O. Chipara, C. Lu, T. C. Bailey, and G.-C. Roman, "Reliable clinical monitoring using wireless sensor networks: Experiences in a step-down hospital unit," in *ACM SenSys*, 2010.
- [10] K. Lorincz, D. Malan, T. Fulford-Jones, A. Nawoj, A. Clavel, V. Shnayder, G. Mainland, M. Welsh, and S. Moulton, "Sensor networks for emergency response: challenges and opportunities," *IEEE Trans. Pervasive Computing*, 3(4), pp. 16–23, Oct 2004.
- [11] X. Li, R. Falcon, A. Nayak, and I. Stojmenovic, "Servicing wireless sensor networks by mobile robots," *IEEE Comm. Mag.*, 50(7), 2012.
- [12] Y. Pei and M. W. Mutka, "Stars: Static relays for multi-robot real-time search and monitoring," in *IEEE DCOSS*, 2011.
- [13] H. Fotouhi, M. Zuniga, M. Alves, A. Koubaa, and P. Marrón, "Smart-hop: A reliable handoff mechanism for mobile wireless sensor networks," in *EWSN*, 2012.
- [14] H. Fotouhi, M. Alves, M. Zuniga, and A. Koubaa, "Reliable and fast hand-offs in low-power wireless networks (extended paper)," Tech. Rep., 2014. [Online]. Available: <http://www.cister.isep.ipp.pt/docs/reliable+and+fast+hand%252Doffs+in+low%252Dpower+wireless+networks++%2528extended+paper%2529/825/view.pdf>
- [15] M. Zuniga, I. Irzynska, J. Hauer, T. Voigt, C. Boano, and K. Roemer, "Link quality ranking: Getting the best out of unreliable links," in *IEEE DCOSS*, 2011.
- [16] N. Baccour, A. Koubaa, L. Mottola, M. Zúñiga, H. Youssef, C. Boano, and M. Alves, "Radio link quality estimation in wireless sensor networks: a survey," *ACM Trans. Sensor Networks*, 8(4), pp. 34:1–34:33, 2012.
- [17] A. Woo, T. Tong, and D. Culler, "Taming the underlying challenges of reliable multihop routing in sensor networks," in *ACM SenSys*, 2003.
- [18] L. Mottola, G. P. Picco, M. Ceriotti, S. Guna, and A. L. Murphy, "Not all wireless sensor networks are created equal: A comparative study on tunnels," *ACM Trans. Sensor Networks*, 7(2), pp. 15:1–15:33, 2010.
- [19] B. Kusy, C. Richter, W. Hu, M. Afanasyev, R. Jurdak, M. Brunig, D. Abbott, C. Huynh, and D. Ostry, "Radio diversity for reliable communication in wsns," in *ACM/IEEE IPSN*, 2011.
- [20] M. Zuniga and B. Krishnamachari, "Analyzing the transitional region in low power wireless links," in *IEEE SECON*, 2004.
- [21] M. Zúñiga and B. Krishnamachari, "An analysis of unreliability and asymmetry in low-power wireless links," *ACM Trans. Sensor Networks*, 3(2), pp. 1–34, 2007.
- [22] J. Polastre, R. Szewczyk, and D. Culler, "Telos: enabling ultra-low power wireless research," in *ACM/IEEE IPSN*, 2005.
- [23] T. Rappaport, *Wireless communications: principles and practice*. IEEE press, 1996.
- [24] N. Alam, A. Balaie, and A. Dempster, "Dynamic path loss exponent and distance estimation in a vehicular network using doppler effect and received signal strength," in *IEEE VTC*, 2010.
- [25] M. Thamri, "Evaluation of smart-hop: a handoff approach for mobile wireless sensor networks," Master's thesis, Higher School of Communication of Tunis, Sup'Com, 2012.
- [26] R. Fish, M. Flickinger, and J. Lepreau, "Mobile emulab: A robotic wireless and sensor network testbed," in *IEEE INFOCOM*, 2006.
- [27] O. Rensfelt, F. Hermans, P. Gunningberg, L. Larzon, and E. Björnemo, "Repeatable experiments with mobile nodes in a relocatable wsn testbed," *The Computer Journal*, 54(12), 2011.
- [28] S. Cho, E. Jang, and J. Cioffi, "Handover in multihop cellular networks," *IEEE Comm. Mag.*, 47(7), 2009.
- [29] T. Salih and K. Fidanboylyu, "Modeling and analysis of queuing handoff calls in single and two-tier cellular networks," *Computer Communications*, 29(17), 2006.
- [30] B. Madan, S. Dharmaraja, and K. Trivedi, "Combined guard channel and mobile-assisted handoff for cellular networks," *IEEE Trans. Vehicular Tech.*, 57(1), 2008.
- [31] I. Ramani and S. Savage, "Synscan: practical fast handoff for 802.11 infrastructure networks," in *IEEE INFOCOM*, 2005, pp. 675–684 vol. 1.
- [32] A. Mishra, M. Shin, and W. Arbaugh, "An empirical analysis of the ieee 802.11 mac layer handoff process," *ACM SIGCOMM*, 2003.
- [33] M. Shin, A. Mishra, and W. A. Arbaugh, "Improving the latency of 802.11 hand-offs using neighbor graphs," in *ACM MobiSys*, 2004.
- [34] J. Petajajarvi and H. Karvonen, "Soft handover method for mobile wireless sensor networks based on 6lowpan," in *IEEE DCOSS*, 2011.
- [35] Z. Zinonos and V. Vassiliou, "S-ginmob: Soft-handoff solution for mobile users in industrial environments," in *IEEE DCOSS*, 2011.
- [36] D. De Couto, D. Aguayo, J. Bicket, and R. Morris, "A high-throughput path metric for multi-hop wireless routing," in *ACM MobiCom*, 2003.
- [37] N. Baccour, A. Koubaa, H. Youssef, M. Ben Jamaa, D. do Rosário, M. Alves, and L. Becker, "F-lq: A fuzzy link quality estimator for wireless sensor networks," in *EWSN*, 2010.



Hossein Fotouhi is a Ph.D. student at CISTER/INESC-TEC Research Unit and University of Porto, working in the areas of sensor networks, mobile computing and Internet of Things. In 2009, he completed Master of Science at University Putra Malaysia on Communication Network Engineering. In 2004, he obtained Bachelor of Science at University of Guilan on Electrical Electronics Engineering. He worked 3 years afterward in industry as a network engineer.



Mário Alves has a PhD (2003) in ECE at the University of Porto, Portugal. He is a Professor in ECE at Politécnico do Porto (ISEP/IPP) and a Research Associate at the CISTER/INESC-TEC Research Unit, a top-ranked Portuguese research centre. His current research interests are mainly devoted to quality-of-service (QoS) in low-power wireless networks, particularly concerning timeliness and reliability issues.



Marco Zúñiga Zamalloa is an Assistant Professor in the Department of Computer Science at Delft University of Technology, the Netherlands. He obtained his PhD and MSc in Electrical Engineering from the University of Southern California, in 2002 and 2006, respectively; and his BSc in Electronics Engineering from the Pontificia Universidad Católica del Perú. His research interest are in the areas of wireless networks, pervasive computing and cyber physical systems.



Anis Koubaa is currently an Associate Professor in Computer Science at Prince Sultan University and Senior Research Associate at the CISTER/INESC-TEC Research Unit. He has a PhD (2004) in Computer Science from INPL Lorraine, France. He edited and authored more than 4 books, 90 journal and conference papers. He received the award of the Best Research Work competition from Al-Imam University in 2010. His research interests are mobile robots and sensor networks.